AGU PUBLICATIONS

JGR

Journal of Geophysical Research: Space Physics

RESEARCH ARTICLE
10.1002/2015JA021310

Key Points:
- Bottomside ionosphere made a minor contribution to ionospheric positive storm
- TEC changes are not necessarily related to ionospheric peak densities
- TEC increases are also associated with effective plasma scale height variations

Correspondence to:
J. Lei,
leijh@ustc.edu.cn

Citation:
Lei, J., Q. Zhu, W. Wang, A. G. Burns, B. Zhao, X. Luan, J. Zhong, and X. Dou (2015), Response of the topside and bottomside ionosphere at low and middle latitudes to the October 2003 superstorms, *J. Geophys. Res. Space Physics*, *120*, 6974–6986, doi:10.1002/2015JA021310.

Received 7 APR 2015
Accepted 7 JUL 2015
Accepted article online 14 JUL 2015
Published online 19 AUG 2015

Response of the topside and bottomside ionosphere at low and middle latitudes to the October 2003 superstorms

Jiuhou Lei[1], Qingyu Zhu[1], Wenbin Wang[2], Alan G. Burns[2], Biqiang Zhao[3], Xiaoli Luan[1], Jiahao Zhong[1], and Xiankang Dou[1]

[1]CAS Key Laboratory of Geospace Environment, University of Science and Technology of China, Hefei, China, [2]High Altitude Observatory, National Center for Atmospheric Research, Boulder, Colorado, USA, [3]Institute of Geology and Geophysics, Chinese Academy of Sciences, Beijing, China

Abstract Ionospheric observations from the ground-based GPS receiver network, CHAMP and GRACE satellites and ionosondes were used to examine topside and bottomside ionospheric variations at low and middle latitudes over the Pacific and American sectors during the October 2003 superstorms. The latitudinal variation and the storm time response of the ground-based GPS total electron content (TEC) were generally consistent with those of the CHAMP and GRACE up-looking TEC. The TECs at heights below the satellite altitudes during the main phases were comparable to, or even less than, the quiet time values. However, the storm time CHAMP and GRACE up-looking TECs showed profound increases at low and middle latitudes. The ground-based TEC and ionosonde data were also combined to study the TEC variations below and above the F_2 peak height (h_mF_2). The topside TECs above h_mF_2 at low and middle latitudes showed significant increases during storm time; however, the bottomside TEC below h_mF_2 did not show so obvious changes. Consequently, the bottomside ionosphere made only a minor contribution to the ionospheric positive phase seen in the total TEC at low and middle latitudes. Moreover, at middle latitudes F_2 peak electron densities during storm time did not have the obvious enhancements that were seen in both the ground-based and topside TECs, although they were accompanied by increases of h_mF_2. Therefore, storm time TEC changes are not necessarily related to changes in ionospheric peak densities. Our results suggest that TEC increases at low and middle latitudes are also associated with effective plasma scale height variations during storms.

1. Introduction

The interactions between coronal mass ejections and the Earth's magnetosphere generated several geomagnetic storms at the end of October 2003 when the Sun was extremely active [*Gopalswamy et al.*, 2005]. The meridional component of the interplanetary magnetic field (IMF B_z) turned southward and stayed southward for a long period of time on 30 and 31 October. As a result, the ring current index, *Dst*, had sharp decreases on both days and reached two minima of about −360 nT and −400 nT in the two superstorms (see Figure 1). Many studies were devoted to examining the response of the ionosphere and thermosphere system to these two superstorms [*Abdu et al.*, 2007, 2008; *Anderson et al.*, 2006; *Batista et al.*, 2006; *Balan et al.*, 2011; *Basu et al.*, 2005, 2007; *Foster and Rideout*, 2005; *Lin et al.*, 2005a, 2005b; *Lei et al.*, 2011, 2012, 2014; *Liu and Lühr*, 2005; *Mannucci et al.*, 2005; *Sahai et al.*, 2005; *Sutton et al.*, 2005; *Tsurutani et al.*, 2007, 2008; *Yizengaw et al.*, 2005; *Zhao et al.*, 2005].

This is a follow-up to the study of *Lei et al.* [2014]. They used ionospheric observations from multiple low Earth orbit (LEO) satellites and investigated the ionospheric response to these two superstorms over the Pacific and American sectors. Satellite total electron content (TEC) profiles revealed substantial increases in TEC in the daytime at low and middle latitudes during both superstorms. However, the up-looking TECs did not provide information about the changes in electron densities below the satellite altitudes. In this study, we use ground-based GPS TEC in conjunction with CHAMP and GRACE up-looking TECs to examine whether the enhancements of the up-looking TEC are consistent with those of the ground-based TEC observations.

Ground-based TEC is widely used to describe the total ionization of the ionosphere, while the up-looking TEC of LEO satellite gives the state of the topside ionosphere above the satellite orbits. Hence, we can obtain the

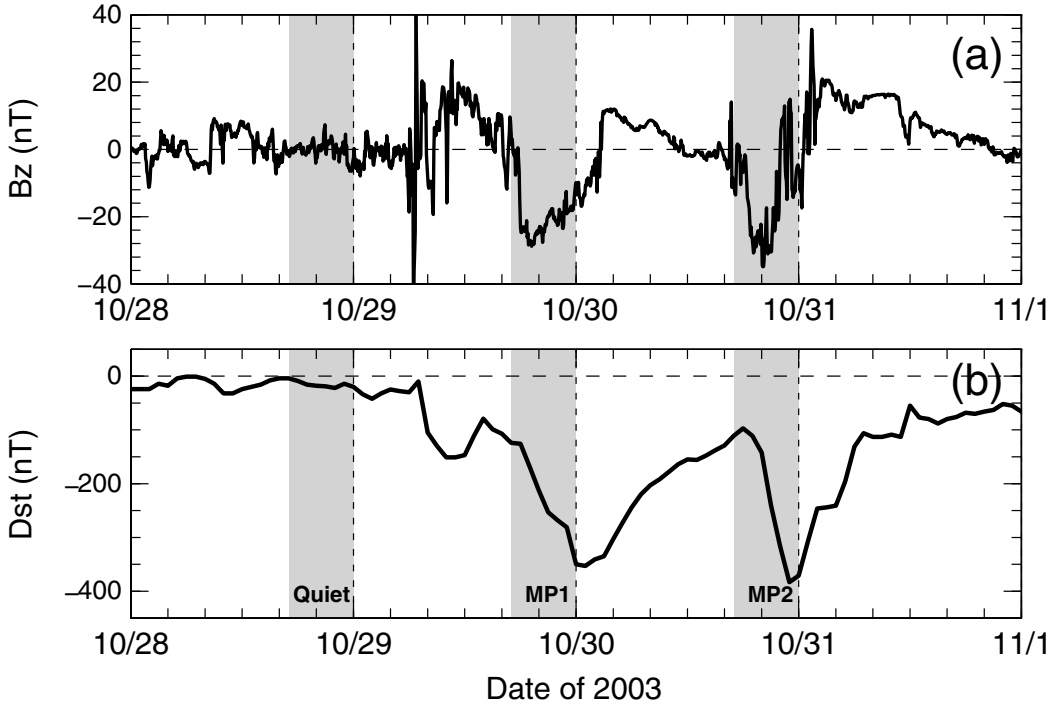

Figure 1. Variations of (a) the north-south component of the interplanetary magnetic field (IMF B_z) observed by the ACE satellite and (b) *Dst* during 28–31 October 2003. The three shaded time intervals are the periods in which we are interested.

TECs above and below the CHAMP and GRACE satellite altitudes by combining ground-based and LEO-based TECs. Meanwhile, the TECs above and below the F_2 peak height at low- and middle-latitude ionosonde stations are calculated using ionosonde observations of ionospheric density profiles up to the F_2 peak. Ground-based TECs at the same locations were used to provide additional information about the storm time evolution of the topside and bottomside ionosphere. Therefore, another and the primary objective of this study is to explore whether the response to the October 2003 storms was different in the daytime topside and bottomside ionosphere, by combining the observations from the ground-based GPS receiver network, CHAMP and GRACE satellites and ionosondes over the Pacific and American sectors. We also investigated the possible different low and middle latitude responses of the ionospheric peak density and the topside ionosphere to major geomagnetic storms using this comprehensive data set of both ground- and space-based observations. This kind of study can shed light on the complicated response of the entire ionosphere-thermosphere system to geomagnetic perturbations and the mechanisms that drive this response.

2. Ionospheric Data Set

In this study, TEC observations from the ground-based GPS Receiver Network and two LEO satellites (i.e., CHAMP and GRACE) were the main data sources used. The TEC derivations were examined for both ground-based receivers [e.g., *Klobuchar*, 1996; *Mannucci et al.*, 1998; *Rideout and Coster*, 2006; *Astafyeva*, 2009] and LEO satellites [e.g., *Yue et al.*, 2011; *Zhong et al.*, 2015]. Due to the dispersive character of the ionosphere, the line of sight TEC from the receiver to the GPS satellite can be measured using the GPS dual-frequency signals [e.g., *Klobuchar*, 1996; *Mannucci et al.*, 1998; *Rideout and Coster*, 2006]. Generally, before processing the GPS data, outliers are eliminated and cycle slips are detected. The relative line of sight TEC can then be obtained after leveling the carrier phase observations to the pseudorange measurements. The GPS satellite biases released by the Global Navigation Satellite Systems (GNSS) community and the estimated receiver bias are first subtracted from the relative TEC to obtain the absolute TEC. The absolute line of sight TEC is then converted to the absolute vertical TEC using a mapping function. The ground-based GPS data were obtained from the Massachusetts Institute of Technology (MIT)

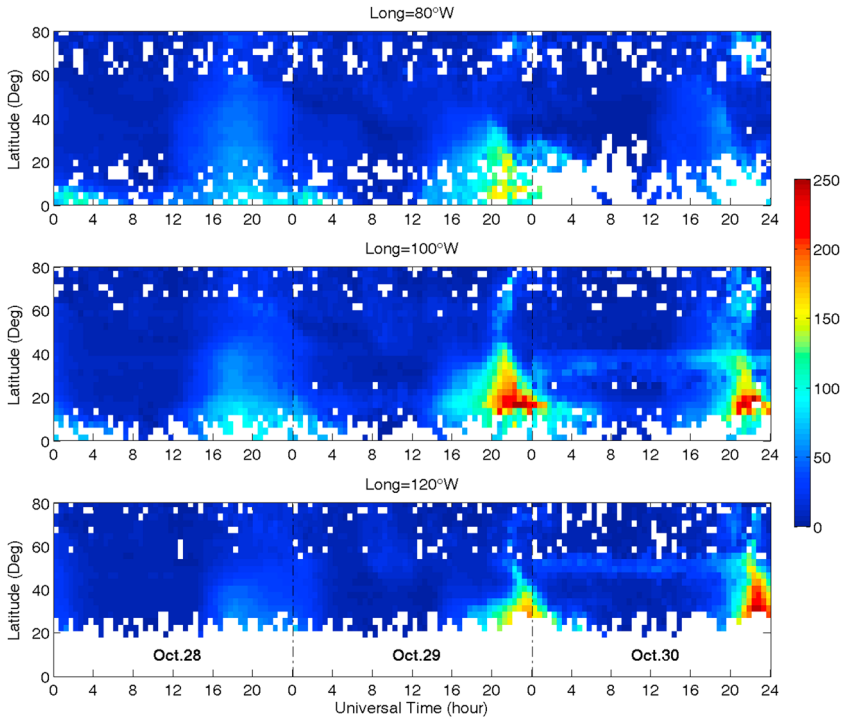

Figure 2. Latitudinal variations of ground-based TEC at different longitudes in the North Hemisphere during 28–30 October, 2003. Top: 80°W; middle: 100°W; bottom: 120°W.

Haystack Observatory Madrigal database (http://madrigal.haystack.mit.edu/). A detailed description for the LEO TEC retrieval can be found in *Lei et al.* [2014]. During this study period, CHAMP and GRACE flew at ~400 and 500 km, respectively, and the local times were 12:57/00:58 LT for CHAMP and 15:52/03:53 LT for GRACE in low and middle latitudes. CHAMP and GRACE data on the dayside were used in this study.

We also used simultaneous ionosonde data from four stations in the American sector: Dyess (32.4°N, 99.8°W; magnetic latitude (MLAT) 41.4°N, magnetic longitude (MLON) 32.0°W), Eglin (30.5°N, 86.5°W; MLAT 40.4°N, MLON 16.8°W), Ramey (18.5°N, 67.1°W; MLAT 28.8°N, MLON 5.0°E), and Jicamarca (12°S, 76.8°W; MLAT 1.7°S, MLON 5.0°W). The ionospheric peak height (h_mF_2) and peak density (N_mF_2) along with the integrated electron content below the F_2 peak, namely, the bottomside TEC, were used to further provide information about ionospheric densities in the F_2 layer.

In order to investigate the respective evolution of the topside and bottomside ionosphere during storm times, the differences between the ground-based TEC and up-looking TECs from CHAMP and GRACE were utilized to give the TEC below the satellite orbits. We call these TEC differences as down-looking TEC to distinguish them from the ionosonde bottomside TEC. Additionally, the difference between GPS TEC and ionosonde bottomside TEC stands for the TEC above the F_2 peak, which is designated the topside TEC in our study.

3. Observations and Results

The CHAMP and GRACE up-looking TECs in *Lei et al.* [2014] showed significant increases during the two main phases. However, the LEO observations only provided TEC values above the satellite altitudes. In this study, we combined the ground-based and LEO-based TECs to explore the topside and bottomside ionospheric response to the October 2003 superstorms. Before doing that, we analyzed the variations of ground-based GPS TEC profiles in the Pacific and American sectors. As shown in Figure 2, the daytime ground-based GPS TEC at 80°W–120°W during quiet time was about 70–100 total electron content unit (TECU, 1 TECU = 10^{16} el m^{-2}) at low latitudes, which was probably associated with the equatorial ionization anomaly (EIA) crest, and 30–40 TECU at middle and high latitudes. However, during storm time, significant increases

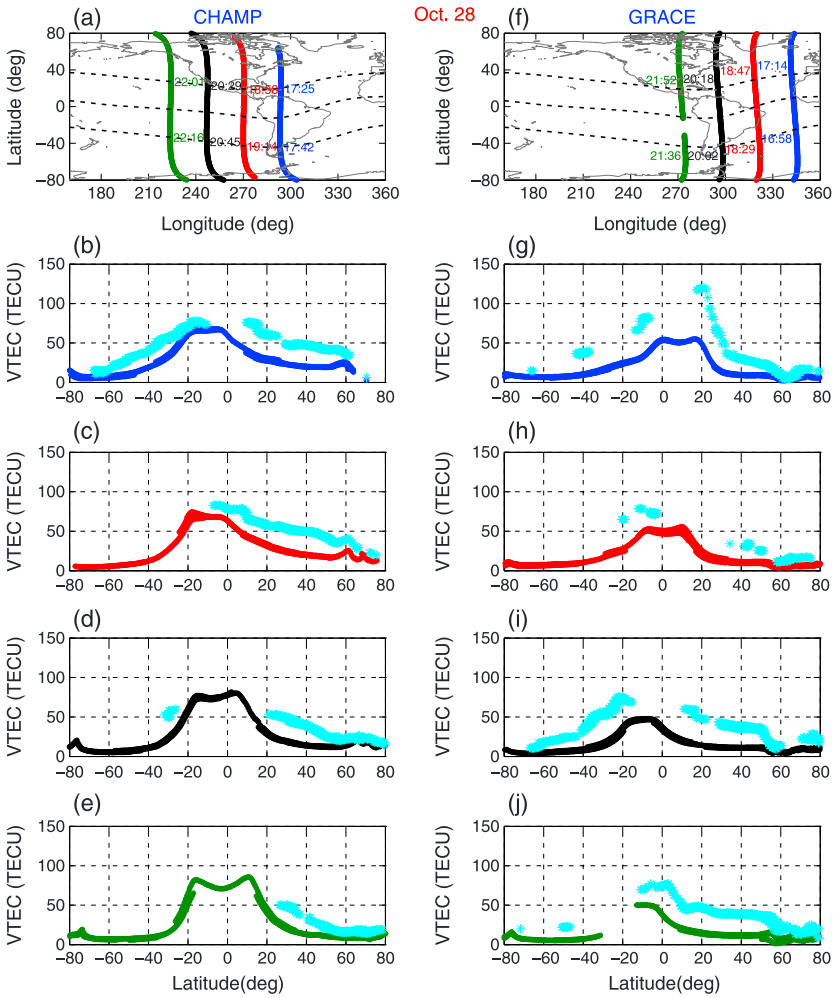

Figure 3. Comparison of the up-looking TECs from (b–e) CHAMP and (g–j) GRACE satellites with ground-based TECs (cyan) sampled along the LEO satellite orbits during the quiet time on 28 October 2003. The corresponding satellite orbits are shown in Figures 3a and 3f, in which the dashed lines represent the magnetic dip equator and geomagnetic latitudes of 30°N and 30°S. The UTs when the satellite passed over the magnetic latitudes of 30°N and 30°S for each orbit are also given.

occurred at low and middle latitudes. During the main phase on 29 October (MP1), TEC reached ~160 TECU at 80°W, and it was even greater at 100°W and 120°W. At 100°W, the maximum of TEC reached about 280 TECU, and the increase extended to a latitude of 50°N. It is also noticeable that the increase of TEC was seen from 20°N to 40°N at 120°W. During the main phase on 30 October (MP2), the increase was slightly weaker than during MP1 at 80°W and 100°W, although no data were available at low latitudes at 80°W. At 120°W, substantial increases in TEC were observed from 20°N to 40°N, and the enhancements were stronger than those during MP1. In addition to the prominent enhancements at low and middle latitudes, strong increases of TEC also extended to higher latitudes during both MP1 and MP2, particularly at 100°W and 120°W. *Chi et al.* [2005] and *Lin et al.* [2005a] demonstrated that this feature could be associated with the ionospheric TEC plume, an ionospheric signature of the plasmaspheric tail [*Foster et al.*, 2002]. As revealed in *Lei et al.* [2014], the different ionospheric response at different longitudes was related to local time differences in the upward plasma drift.

Given that ground-based GPS TEC showed a similar increase during the two main phases to that seen in the LEO-based up-looking TEC, we further compared the up-looking TEC with ground-based GPS TEC along the satellite orbits during the three time intervals in which we were interested (Figure 1). Figure 3 shows a comparison of CHAMP and GRACE up-looking TECs with ground-based TECs during quiet time on 28 October 2003. The ground-based TECs were sampled along the LEO satellite orbits at the

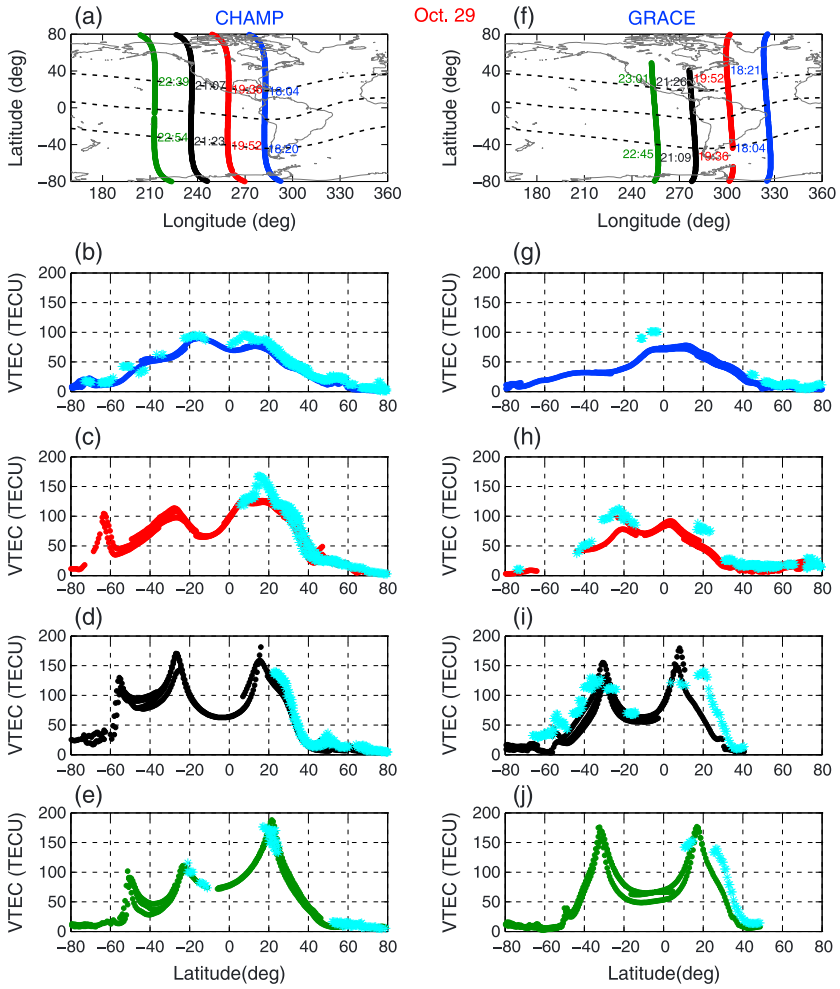

Figure 4. Comparison of the up-looking TEC from (b–e) CHAMP and (g–j) GRACE satellites with ground-based TECs (cyan) sampled along the LEO satellite orbits during the main phase of the 29 October superstorm (MP1). The corresponding satellite orbits are shown in Figures 3a and 3f, in which the dashed lines represent the magnetic dip equator and geomagnetic latitudes of 30°N and 30°S. The UTs when the satellite passed over the magnetic latitude 30°N and 30°S for each orbit are also given.

ionospheric pierce point, the intersection between the slant GNSS signal raypath and the ionospheric spherical shell. As shown in this figure, the CHAMP up-looking TECs were larger by about 20–30 TECU than the GRACE TECs, since the GRACE satellite flew about 100 km higher than the CHAMP satellite. Clearly, the CHAMP and GRACE up-looking TECs were greater at the equatorial and low latitudes than at high latitudes. The maximum TECs for CHAMP and GRACE data were about 80 and 60 TECU, respectively. For ground-based TEC profiles (cyan dots), the latitudinal variations were generally consistent with those of the up-looking TECs for both CHAMP and GRACE, although the ground-based TECs were larger than the LEO up-looking TECs.

Figures 4 and 5 show the comparison between CHAMP and GRACE up-looking TECs and the ground-based GPS TECs during two main phases of the October storms. Both CHAMP and GRACE up-looking TECs had significant increases, with obvious EIA features, during storm time. Additionally, during MP2 the CHAMP up-looking TEC (Figures 5c and 5d) had a more significant absolute increase than the GRACE up-looking TEC (Figures 5g and 5h). Consequently, the maximum of CHAMP up-looking TEC during MP2 was much larger than during MP1, whereas GRACE up-looking TECs during two main phases were comparable. As suggested by *Lei et al.* [2014], the local time differences in the CHAMP and GRACE TEC enhancements are attributed to the corresponding differences in the upward vertical drifts that were observed by the ROCSAT satellite.

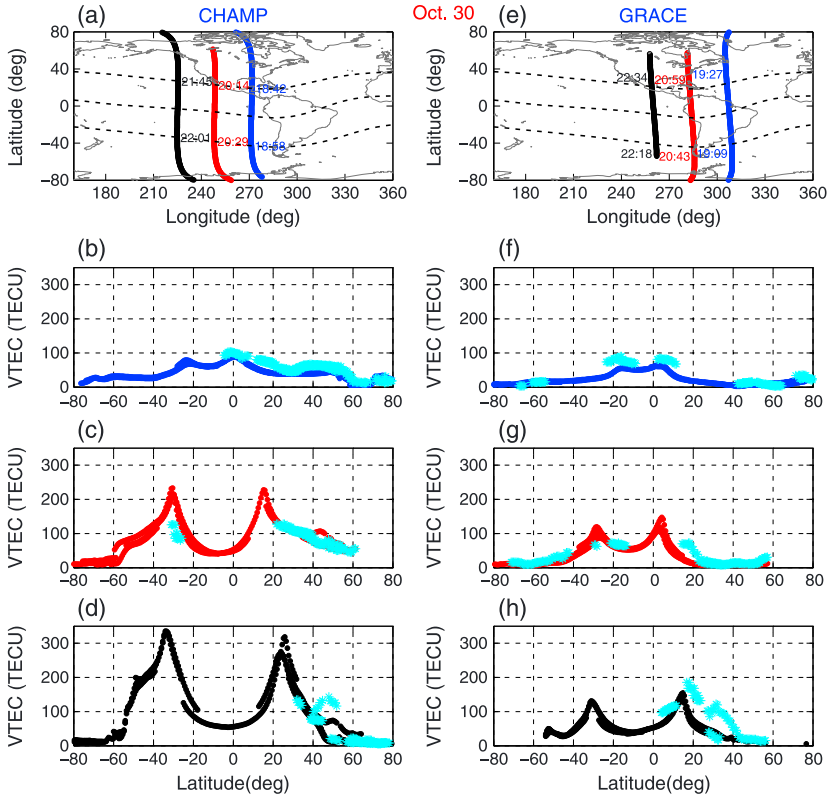

Figure 5. Comparison of the up-looking TEC from (b–d) CHAMP and (f–h) GRACE satellites with ground-based TECs (cyan) sampled along the LEO satellite orbits during the main phase of the 30 October superstorm (MP2). The corresponding satellite orbits are shown in Figures 3a and 3f, in which the dashed lines represent the magnetic dip equator and geomagnetic latitudes of 30°N and 30°S. The UTs when the satellite passed over the magnetic latitude of 30°N and 30°S for each orbit are given.

In Figures 4 and 5, the ground-based TECs during the two main phases tracked the latitudinal variation and the storm response seen in the LEO-based up-looking TECs well. The differences between the ground-based and LEO-based TECs were still obvious before the storm onset, whereas they became relatively less prominent during the main phase. Besides the EIA features, the observed enhancements in the LEO-based TECs were also seen in the ground-based TECs at middle and higher latitudes. For example, larger ground-based GPS TEC bumps occurred at 54°S at 21:07 UT (Figure 4i) and 48°N at about 21:40 UT (Figure 5d).

To quantitatively show the ionospheric response below the LEO orbits, we calculated the differential value between ground-based GPS TEC and LEO up-looking TEC; this value is referred to as down-looking TEC. Figures 6a–6c show the variations of the TEC below CHAMP (CHAMP down-looking TEC) during 28–30 October. As shown in Figures 6a, the CHAMP down-looking TECs were less than 45 TECU during quiet time. Interestingly, there were weak double-crest latitudinal structures. This indicates that the F_2 peak height was beneath the CHAMP satellite. During the main phases on 29 and 30 October (Figures 6b and 6c), the CHAMP down-looking TECs were even smaller than during the quiet time. This implies that the F_2 peak height was lifted to such an extent that it reached an altitude near or above the CHAMP altitude, as we will discuss later.

Figures 6d–6f display the variation of TEC below GRACE (GRACE down-looking TEC) during 28–30 October. It is also clear that during quiet time, in Figures 3g–3j the GRACE down-looking TEC was generally lower than ~55 TECU, with the exception of the orbit at around 17:00–18:00 UT, when the maximum down-looking TEC reached 81 TECU. This is probably associated with longitudinal variations in the ionosphere. Note that the GRACE down-looking TEC was greater than the CHAMP down-looking TEC due to the higher orbital altitude of the GRACE satellite. During quiet time, the GRACE down-looking TEC was comparable to, or slightly lower than, the up-looking TEC. However, during storm time, the GRACE down-looking TEC did

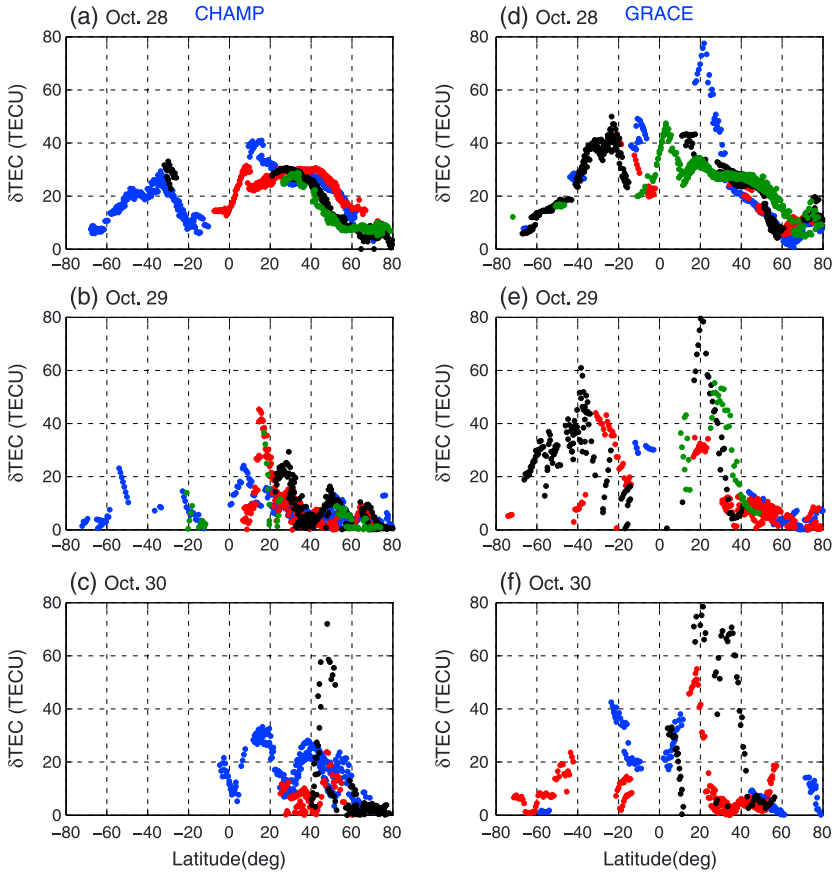

Figure 6. Differences between ground-based GPS and up-looking TECs for each orbit during quiet time and the two main phases of the storms. (a–c) CHAMP; (d–f) GRACE. Different colors represent the TEC data along different orbits in Figures 3–5. Note that only are positive differential TECs shown here, although the ground-based TECs are occasionally smaller than the up-looking TECs.

not significantly change, whereas the up-looking TEC increased greatly at low and middle latitudes (right columns in Figures 4 and 5). As a result, during storm time the GRACE down-looking TEC was much smaller than the up-looking TEC. In addition, the double-crest feature occurred during both quiet and storm times. Again, this demonstrated that the GRACE down-looking TEC were mostly determined by the electron densities near the F_2 peak region below the satellite.

The results in Figures 2–6 indicate that the increase of the ionosphere TEC above the satellite orbits during the October 2003 storms was the main cause of the positive storm effect seen in the ground-based GPS TEC, given that the ionosphere below the satellite orbits did not significantly change during this time. However, it should be pointed out that the LEO satellites only provided up-looking TEC observations above their orbital altitudes. Next, we use ionosonde data from Dyess, Eglin, Ramey, and Jicamarca to provide more information about the evolution of the topside and bottomside ionosphere during storm time.

Figure 7 shows the variations of ground-based GPS TEC, bottomside TEC, and topside TEC at four ionosonde stations during 28–30 October. In daytime, the bottomside TEC was ~20 TECU and the topside TEC was greater than the bottomside TEC by a factor of 2–5 with the exception at Jicamarca, in which the topside TEC was comparable to the bottomside TEC. At the low and middle latitudinal stations (Dyess, Eglin, and Ramey), both the ground-based GPS TEC and topside TEC showed significant increases, except that at Eglin the ground-based GPS and topside TECs did not show such changes during MP2. The different topside ionosphere responses to the storms at Dyess and Eglin are consistent with the results in Figure 2.

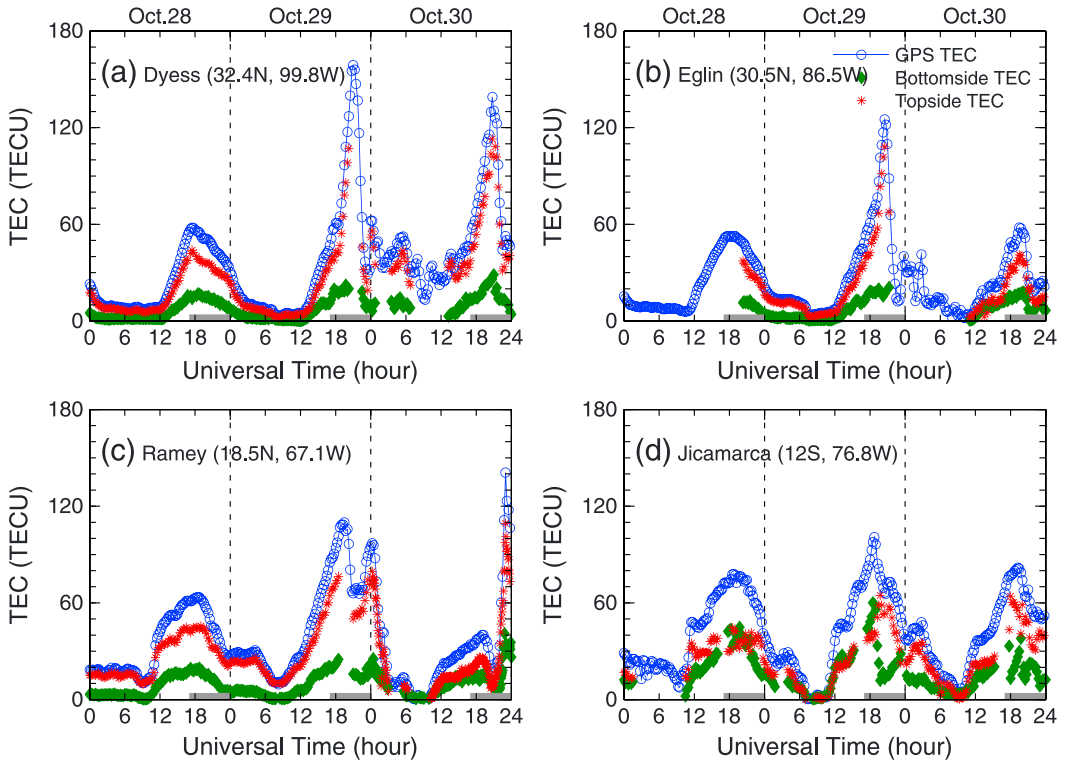

Figure 7. Comparison of ground-based bottomside and topside TECs at Dyess, Eglin, Ramey, and Jicamarca during 28–30 October, 2003. The blue lines with circles represent the ground-based GPS TEC; the green diamond lines denote the bottomside TEC below the F_2 peak height calculated from ionosonde measurements, and the red asterisks represent the topside TEC (the difference between GPS TEC and bottomside TEC).

Figure 8 depicts the absolute changes of the storm time ground-based GPS TEC, bottomside TEC, and topside TEC at these four ionosonde stations compared with the prestorm TECs. Note that in order to obtain the bottomside TEC changes, the ionosonde data gap before 20:00 UT on 28 October at Eglin was filled by the quiet time values at Dyess. This is an appropriate substitution as these two stations are close and they share similar quiet time, ionospheric structure. Clearly, the storm time changes in the bottomside TEC were much smaller than those in the topside TEC at the low and middle latitudinal stations (Dyess, Eglin, and Ramey), so that the topside TEC approximated the ground-based GPS TEC (the total TEC) during storms. At these three stations, both ground-based GPS TEC and topside TEC showed significant increases, except that at Eglin the ground-based GPS TEC and topside TEC during MP2 underwent a slight decrease. Overall, the bottomside TEC during storm time at these three stations did not show such a significant increase relative to the quiet time reference data, except at Ramey during late MP2, when the increase of the bottomside TEC reached about 40 TECU. At Jicamarca, an equatorial station, the ground-based GPS TEC, bottomside TEC, and topside TEC did not show the strong changes seen at the other three stations. In summary, increases in the low- and middle-latitude topside ionosphere were prominent during the October 2003 superstorms, and the bottomside ionosphere only made minor contributions to the observed ionospheric positive phase in the total TEC at low and middle latitudes.

4. Discussion

In this study, the ground-based GPS TEC, up-looking TEC from CHAMP and GRACE, and bottomside TEC derived from ionosonde observations were used to study the different responses of the topside and bottomside ionosphere to the October 2003 storms. It was found that during the main phases of the storms, the bottomside TEC at low and middle latitudes comprised a much smaller portion of the total TEC compared with its influence during the quiet time reference period. The topside TEC was comparable to the total TEC in the storm period, and a significant enhancement of TEC occurred in the topside

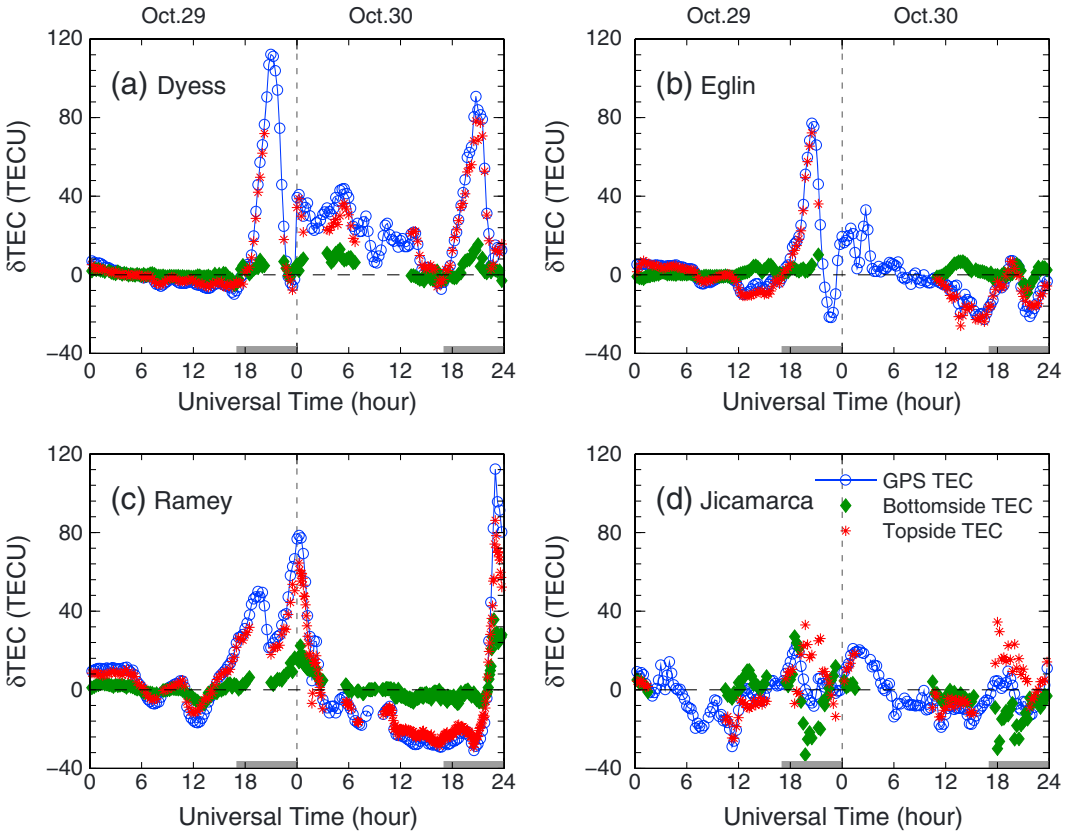

Figure 8. Changes of ground-based bottomside and topside TECs between storm time on 29 and 30 October and quiet time at Dyess, Eglin, Ramey, and Jicamarca.

ionosphere. Near the equator, the topside TEC tended to be comparable to the bottomside TEC in the main phases of the storms. No significant enhancement of TEC occurred in the topside ionosphere at these latitudes. *Zhao et al.* [2012] used the ground-based GPS TEC and bottomside TEC from the ionosonde data to examine the ionosphere response to the 20–22 November 2003 storm, and they also indicated that the bottomside ionosphere did not significantly change during storm time. Besides the combination of ground-based GPS TEC and ionosonde data, we compared the LEO-based TEC with the ground-based TEC along the LEO satellite path for each orbit. We found a good consistency between the upward looking TEC and the ground-based TEC during the October 2003 storms. By combining the ground-based and LEO-based TECs, we also found that the TEC below the orbits of the LEO CHAMP and GRACE satellites did not show a significant enhancement during the main phases of the October 2003 storms, whereas TEC above the altitude of the CHAMP and GRACE satellites showed strong increases, which suggests that the main response to the geomagnetic storms took place in the topside ionosphere above the satellite orbital heights during these events.

The remaining question is what were the causes of the increases of TEC in the low- and middle-latitude topside ionosphere during these two superstorms? Before addressing this question, we analyzed the characteristic parameters of the F_2 layer, the peak density (N_mF_2), and the peak height (h_mF_2), which can provide some information about ionospheric dynamical processes. As shown in Figure 9, at Dyess and Eglin, N_mF_2 during the main phases did not show the significant increase seen in both the topside TEC and total TEC. However, h_mF_2 at these two stations was considerably higher. The F_2 peak had been uplifted by about 130 km at these two stations. At Ramey (Figure 9c), N_mF_2 during storm time had a prominent increase and h_mF_2 increased by 120 km during MP1 and 200 km during MP2. At Jicamarca, N_mF_2 had a slight decrease during storm time, whereas h_mF_2 had been uplifted from 360 km to nearly 700 km. Note that the storm time h_mF_2s at these stations reached the heights near or above the CHAMP orbital altitude.

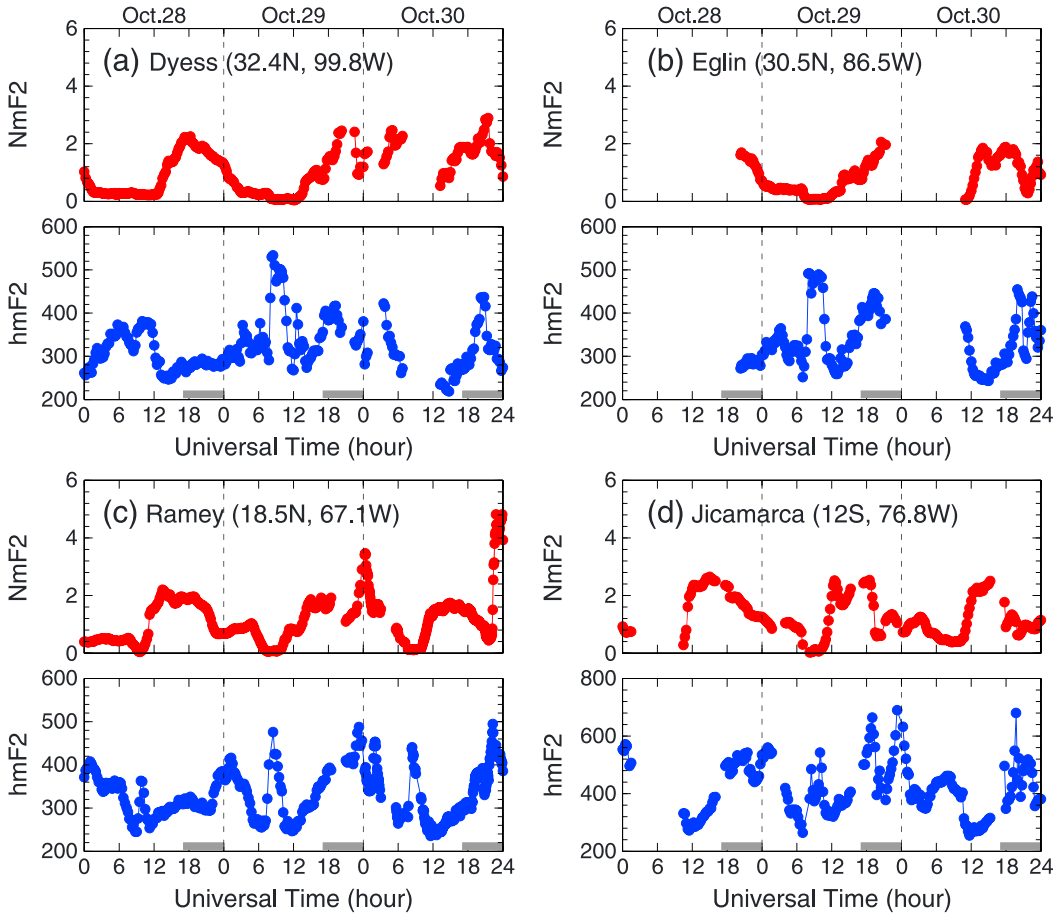

Figure 9. Evolution of the peak density N_mF_2 (in units of 10^{12} m^{-3}) and peak height h_mF_2 (in units of kilometer) obtained from the ionosonde measurements at Dyess, Eglin, Ramey, and Jicamarca during 28–30 October 2003. The intervals on which we focused are marked by the gray bars.

Referring back to Figure 7, during quiet time the topside TECs at low and middle latitudes were larger than the bottomside TECs, which indicates that the thickness of the topside ionosphere is greater than that of the bottomside ionosphere in this region. Thus, during storm time, even though the ionosphere thickness is not altered, the absolute TEC change in the topside ionosphere would be greater than in the bottomside ionosphere, associated with the change of the N_mF_2 and greater thickness of the topside ionosphere. In Figure 10 we show that the ratios of the storm time TECs and N_mF_2 over four ionosonde stations with respect to the quiet time values in order to address whether the greater changes observed in the topside TEC were related to the changes in N_mF_2 or/and ionospheric thickness, given that $\frac{\sigma TEC}{TEC} = \frac{\sigma NmF_2}{NmF_2} + \frac{\sigma\tau}{\tau}$ (where τ denotes ionospheric thickness). As shown in this figure, the variations of the relative changes in N_mF_2 were generally consistent with those in the bottomside TEC during both quiet and storm time. Additionally, the relative changes in the ionospheric parameters were much larger at night than in the daytime, which was possibly associated with the nighttime low backgrounds. Here we focused on the ionospheric response during MP1 and MP2. As shown in Figure 10, a distinct increase in N_mF_2 was observed at Ramey with a maximum enhancement of a factor of 5–7, which was in accord with the relative enhancements in both the bottomside and topside TECs. In Figure 8, the absolute TEC changes at Ramey were comparable to those at Dyess. However, during MP1 and MP2 the relative TEC changes at Ramey (Figure 10c) were much greater than at Dyess (Figure 10a). This could be due to the fact that the October 2003 storms occurred at evening local times over Ramey, when the prestorm electron density was relatively lower. If the ionospheric response during MP1 and MP2 is considered, the relative increases of N_mF_2 at Dyess (Figure 10a) and at Eglin during MP1 (Figure 10b) were not as strong as those of the TECs, although they were accompanied with the

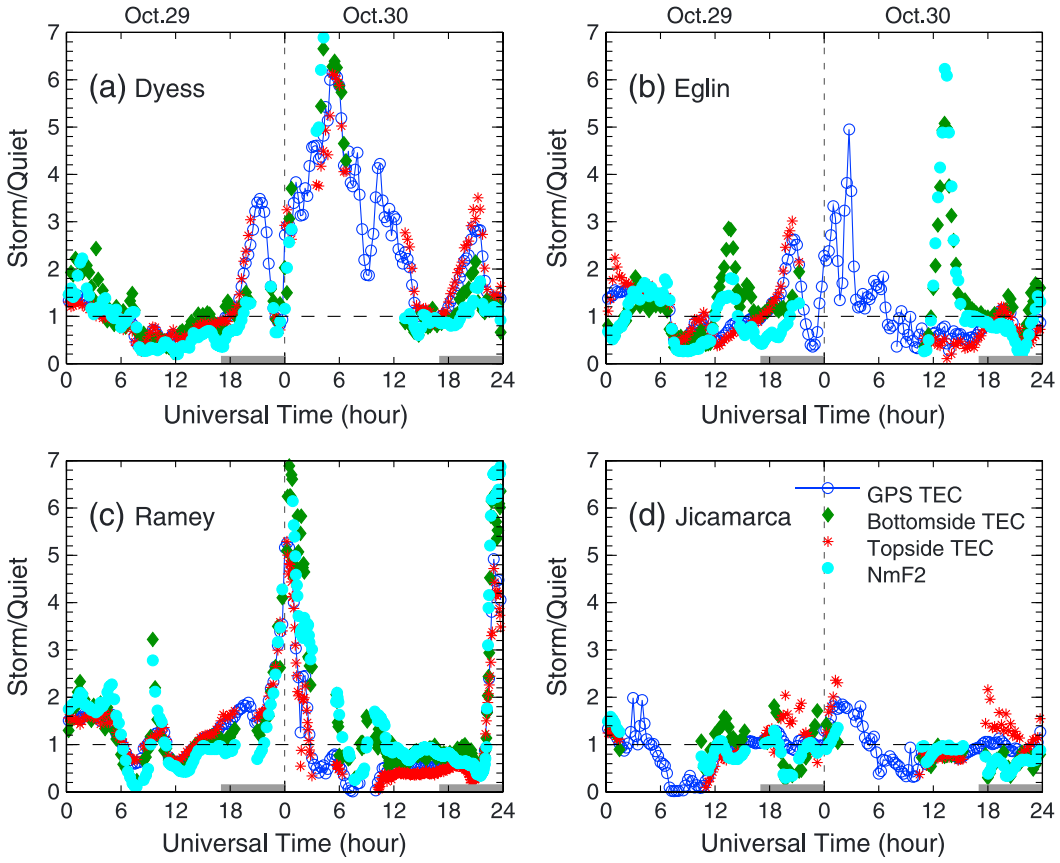

Figure 10. Ratios of the storm time TECs and N_mF_2 on 29 and 30 October to the quiet time values at Dyess, Eglin, Ramey, and Jicamarca. The intervals on which we focused are marked by the gray bars.

increases of h_mF_2. This implies that besides N_mF_2, the topside ionospheric thickness or profile shape had significant changes during the main phases of storms. Thus, the TEC changes seen during storms were not necessarily related to changes in ionospheric peak densities.

As demonstrated by *Lei et al.* [2014], the ROCSAT data showed that a maximum increment of vertical drifts reached 130 m/s at 13:00 LT and 95 m/s at 16:00 LT, associated with prompt penetration electric fields during the two main phases of the October 2003 storms. Thus, the increase of h_mF_2 at low and middle latitudes is consistent with the vertical drift enhancement seen by the ROCSAT satellite. The enhanced daytime electric field tends to move the plasma from the equatorial region into higher latitudes through the fountain effect. Meanwhile, the increased upward vertical drifts also transport local plasma in the bottomside ionosphere or the F_2 layer to higher altitudes where the chemical recombination rate is low, so that plasma accumulates in the topside ionosphere. The plasma transported upward from the bottomside ionosphere would be compensated for by daytime ionization. As a result, the F_2 layer was raised. A large increase was observed in the topside TEC at Dyess during MP1 and MP2 and at Eglin during MP1, although bottomside TEC and N_mF_2 showed a weaker increase at these two stations. This is in accord with the results of *Maruyama et al.* [2004], who showed that increases of the ground-based TEC at middle latitudes over Japan were not reflected in N_mF_2 at the same locations during the November 2001 storm. The increased upward drifts changed the shape of the topside ionosphere (Figure 11 of *Lei et al.* [2014]). Namely, the topside effective plasma scale height $-dh/d(\ln(Ne))$ [*Lei et al.*, 2008], which was most likely associated with this transport process, increased significantly. Our observations are consistent with the simulations reported by *Tsurutani et al.* [2008] and *Huba et al.* [2014]. For the equatorial station Jicamarca, the plasma transported from the bottomside ionosphere was further moved away from the equatorial region, so that the enhanced upward drifts during storm time caused weak positive or negative responses in TEC.

Although the increase of the electric field could be the major contributor to the increases in the topside effective scale height or the topside thickness, the enhanced equatorward wind during storm time should also play an important role in producing changes in electron densities [e.g., *Lin et al.*, 2005b; *Lei et al.*, 2008; *Balan et al.*, 2010]. An equatorward winds can raise the F_2 region to a higher altitude and also tend to counteract field-aligned ambipolar diffusion, thus causing changes in the shape of ionospheric density profile. Conversely, a poleward wind will push the F_2 peak down. Given that these two superstorms happened in October, which is more or less in equinox, the storm-induced wind circulation change should be equatorward and contribute to the enhancement of the topside TEC. However, due to the absence of wind observations, the contribution of neutral winds cannot be evaluated.

As discussed above, ionospheric dynamics mainly contributed to the observed ionospheric positive responses in TEC during the main phases of the October 2003 storms at low and middle latitudes. However, the ionospheric response at different latitude varied, since the response at the equatorial station Jicamarca differed from that of low and middle latitudinal stations. In addition, the evolution of the ionosphere should change with storm phase. At higher latitudes and in the later phases of a storm, thermospheric composition should also play an important role [e.g., *Prölss*, 1995; *Burns et al.*, 1991]. Our further analysis has shown that both the bottomside and topside TEC had a strong depletion at Millstone Hill (42.6°N, 71.5°W; MLAT 52.9°N, MLON 0.3°E), i.e., evident negative phases during the main phases of the October 2003 storms (not shown). This suggests that the bottomside and topside ionospheric response to a storm depends on latitude, longitude, local time, and the storm phase.

5. Summary

In this paper, we focused on describing the response of the topside and bottomside ionosphere at low and middle latitudes to the October 2003 storms by combining ground-based and LEO-based TECs, and ionosonde data. We found that the latitudinal variation and the storm time response of the ground-based GPS TEC were consistent with those of the CHAMP and GRACE up-looking TEC. The TECs below CHAMP and GRACE altitudes occupied a large proportion of the total TEC during quiet time, whereas they became less significant at low and middle latitudes during the main phases of the storms when a strong ionospheric positive phase in TEC occurred. Meanwhile, compared with the prestorm values, the storm time N_mF_2 at middle latitudes had less significant increases that were seen in both the ground-based and topside TECs. This suggests that the TEC change in a storm does not necessarily depend on the storm time behavior of N_mF_2. Furthermore, the bottomside ionosphere was hardly affected by the ionospheric positive TEC phase that occurred in total TEC at low and middle latitudes. Instead, increases of TEC in the topside ionosphere were prominent during the main phases. We suggest that the observed TEC changes at low and middle latitudes are also associated with effective plasma scale height variations due to enhanced prompt penetration electric fields during storm time.

Acknowledgments

The satellite data were provided by UCAR CDAAC (http://cdaac-www.cosmic.ucar.edu/cdaac/) and NASA (ftp://podaac-ftp.jpl.nasa.gov/), ground-based GPS data were obtained from the MIT Haystack Observatory Madrigal database (http://madrigal.haystack.mit.edu/), and the ionosonde data were downloaded from the DIDBase (http://umlcar.uml.edu/). This work was supported by the National Natural Science Foundation of China (41325017, 41274157, 41229001, 41174139, and 41421063), the Project of Chinese Academy of Sciences (KZZD-EW-01), the National Key Basic Research Program of China (2012CB825605), the fundamental research funds for the central universities (WK2080000077), and Thousand Young Talents Program of China. The National Center for Atmospheric Research is sponsored by the National Science Foundation.

Michael Liemohn thanks Smitha Thampi and another reviewer for their assistance in evaluating this paper.

References

Abdu, M. A., T. Maruyama, I. S. Batista, S. Saito, and M. Nakamura (2007), Ionospheric responses to the October 2003 superstorm: Longitude/local time effects over equatorial low and middle latitudes, *J. Geophys. Res.*, *112*, A10306, doi:10.1029/2006JA012228.

Abdu, M. A., et al. (2008), Abnormal evening vertical plasma drift and effects on ESF and EIA over Brazil-South Atlantic sector during the 30 October 2003 superstorm, *J. Geophys. Res.*, *113*, A07313, doi:10.1029/2007JA012844.

Anderson, D., A. Anghel, E. Araujo, V. Eccles, C. Valladares, and C. Lin (2006), Theoretically modeling the low latitude, ionospheric response to large geomagnetic storms, *Radio Sci.*, *41*, RS5S04, doi:10.1029/2005RS003376.

Astafyeva, E. I. (2009), Dayside ionospheric uplift during strong geomagnetic storms as detected by the CHAMP, SAC-C, TOPEX and Jason-1 satellites, *Adv. Space Res.*, *43*, 1749–1756.

Balan, N., K. Shiokawa, Y. Otsuka, T. Kikuchi, D. Vijaya Lekshmi, S. Kawamura, M. Yamamoto, and G. J. Bailey (2010), A physical mechanism of positive ionospheric storms at low latitudes and midlatitudes, *J. Geophys. Res.*, *115*, A02304, doi:10.1029/2009JA014515.

Balan, N., M. Yamamoto, J. Y. Liu, Y. Otsuka, H. Liu, and H. Lühr (2011), New aspects of thermospheric and ionospheric storms revealed by CHAMP, *J. Geophys. Res.*, *116*, A07305, doi:10.1029/2010JA016399.

Basu, S., et al. (2005), Two components of ionospheric plasma structuring at midlatitudes observed during the large magnetic storm of October 30, 2003, *Geophys. Res. Lett.*, *32*, L12S06, doi:10.1029/2004GL021669.

Basu, S., S. Basu, F. J. Rich, K. M. Groves, E. MacKenzie, C. Coker, Y. Sahai, P. R. Fagundes, and F. Becker-Guedes (2007), Response of the equatorial ionosphere at dusk to penetration electric fields during intense magnetic storms, *J. Geophys. Res.*, *112*, A08308, doi:10.1029/2006JA012192.

Batista, I. S., M. A. Abdu, J. R. Souza, F. Bertoni, M. T. Matsuoka, P. O. Camargo, and G. J. Bailey (2006), Unusual early morning development of the equatorial anomaly in the Brazilian sector during the Halloween magnetic storm, *J. Geophys. Res.*, *111*, A05307, doi:10.1029/2005JA011428.

Burns, A. G., T. L. Killeen, and R. G. Roble (1991), A theoretical study of thermospheric composition perturbations during an impulsive geomagnetic storm, *J. Geophys. Res.*, *96*(A8), 14,153–14,167, doi:10.1029/91JA00678.

Chi, P. J., C. T. Russell, J. C. Foster, M. B. Moldwin, M. J. Engebretson, and I. R. Mann (2005), Density enhancement in plasmasphere-ionosphere plasma during the 2003 Halloween Superstorm: Observations along the 330th magnetic meridian in North America, *Geophys. Res. Lett.*, *32*, L03S07, doi:10.1029/2004GL021722.

Foster, J. C., and W. Rideout (2005), Midlatitude TEC enhancements during the October 2003 superstorm, *Geophys. Res. Lett.*, *32*, L12S04, doi:10.1029/2004GL021719.

Foster, J. C., P. J. Erickson, A. J. Coster, J. Goldstein, and F. J. Rich (2002), Ionospheric signatures of plasmaspheric tails, *Geophys. Res. Lett.*, *29*(13), 1623, doi:10.1029/2002GL015067.

Gopalswamy, N., S. Yashiro, Y. Liu, G. Michalek, A. Vourlidas, M. L. Kaiser, and R. A. Howard (2005), Coronal mass ejections and other extreme characteristics of the 2003 October–November solar eruptions, *J. Geophys. Res.*, *110*, A09S15, doi:10.1029/2004JA010958.

Huba, J. D., J. Krall, and S. Sazykin (2014), SAMI3/RCM simulation study of the March 31, 2001 storm, Abstract presented at 2014 Fall Meeting, AGU, San Francisco, Calif., Dec.

Klobuchar, J. A. (1996), Ionospheric effects on GPS, in *Global Positioning System: Theory and Applications*, vol. I, edited by B. W. Parkinson and J. J. Spilker, pp. 485–515, Am. Inst. of Aeronaut. and Astronaut., New York.

Lei, J., W. Wang, A. G. Burns, S. C. Solomon, A. D. Richmond, M. Wiltberger, L. P. Goncharenko, A. Coster, and B. W. Reinisch (2008), Observations and simulations of the ionospheric and thermospheric response to the December 2006 geomagnetic storm: Initial phase, *J. Geophys. Res.*, *113*, A01314, doi:10.1029/2007JA012807.

Lei, J., J. P. Thayer, G. Lu, A. G. Burns, W. Wang, E. K. Sutton, and B. A. Emery (2011), Rapid recovery of thermosphere density during the October 2003 geomagnetic storms, *J. Geophys. Res.*, *116*, A03306, doi:10.1029/2010JA016164.

Lei, J., A. G. Burns, J. P. Thayer, W. Wang, M. G. Mlynczak, L. A. Hunt, X. Dou, and E. Sutton (2012), Overcooling in the upper thermosphere during the recovery phase of the 2003 October storms, *J. Geophys. Res.*, *117*, A03314, doi:10.1029/2011JA016994.

Lei, J., W. Wang, A. G. Burns, X. Yue, X. Dou, X. Luan, S. C. Solomon, and Y. C.-M. Liu (2014), New aspects of the ionospheric response to the October 2003 storms from multiple-satellite observations, *J. Geophys. Res. Space Physics*, *119*, 2298–2317, doi:10.1002/2013JA019575.

Lin, C. H., A. D. Richmond, J. Y. Liu, H. C. Yeh, L. J. Paxton, G. Lu, H. F. Tsai, and S.-Y. Su (2005a), Large-scale variations of the low-latitude ionosphere during the October–November 2003 superstorm: Observational results, *J. Geophys. Res.*, *110*, A09S28, doi:10.1029/2004JA010900.

Lin, C. H., A. D. Richmond, R. A. Heelis, G. J. Bailey, G. Lu, J. Y. Liu, H. C. Yeh, and S.-Y. Su (2005b), Theoretical study of the low- and midlatitude ionospheric electron density enhancement during the October 2003 superstorm: Relative importance of the neutral wind and the electric field, *J. Geophys. Res.*, *110*, A12312, doi:10.1029/2005JA011304.

Liu, H., and H. Lühr (2005), Strong disturbance of the upper thermospheric density due to magnetic storms: CHAMP observations, *J. Geophys. Res.*, *110*, A09S29, doi:10.1029/2004JA010908.

Mannucci, A. J., B. D. Wilson, D. N. Yuan, C. H. Ho, U. J. Lindqwister, and T. F. Runge (1998), A global mapping technique for GPS-derived ionospheric total electron content measurements, *Radio Sci.*, *33*(3), 565–582, doi:10.1029/97RS02707.

Mannucci, A. J., B. T. Tsurutani, B. A. Iijima, A. Komjathy, A. Saito, W. D. Gonzalez, F. L. Guarnieri, J. U. Kozyra, and R. Skoug (2005), Dayside global ionospheric response to the major interplanetary events of October 29–30, 2003 "Halloween Storms", *Geophys. Res. Lett.*, *32*, L12S02, doi:10.1029/2004GL021467.

Maruyama, T., G. Ma, and M. Nakamura (2004), Signature of TEC storm on 6 November 2001 derived from dense GPS receiver network and ionosonde chain over Japan, *J. Geophys. Res.*, *109*, A10302, doi:10.1029/2004JA010451.

Prölss, G. W. (1995), Ionospheric F-region storms, in *Handbook of Atmospheric Electrodynamics*, edited by H. Volland, pp. 195–248, CRC Press, Boca Raton, Fla.

Rideout, W., and A. Coster (2006), Automated GPS processing for global total electron content data, *GPS Solutions*, *10*, 219–228, doi:10.1007/S10291-006-0029-5.

Sahai, Y., et al. (2005), Effects of the major geomagnetic storms of October 2003 on the equatorial and low-latitude F region in two longitudinal sectors, *J. Geophys. Res.*, *110*, A12S91, doi:10.1029/2004JA010999.

Sutton, E. K., J. M. Forbes, and R. S. Nerem (2005), Global thermospheric neutral density and wind response to the severe 2003 geomagnetic storms from CHAMP accelerometer data, *J. Geophys. Res.*, *110*, A09S40, doi:10.1029/2004JA010985.

Tsurutani, B. T., O. P. Verkhoglyadova, A. J. Mannucci, T. Araki, A. Sato, T. Tsuda, and K. Yumoto (2007), Oxygen ion uplift and satellite drag effects during the 30 October 2003 daytime superfountain event, *Ann. Geophys.*, *25*, 569–574.

Tsurutani, B. T., et al. (2008), Prompt penetration electric fields (PPEFs) and their ionospheric effects during the great magnetic storm of 30–31 October 2003, *J. Geophys. Res.*, *113*, A05311, doi:10.1029/2007JA012879.

Yizengaw, E., M. B. Moldwin, P. L. Dyson, and T. J. Immel (2005), Southern Hemisphere ionosphere and plasmasphere response to the interplanetary shock event of 29–31 October 2003, *J. Geophys. Res.*, *110*, A09S30, doi:10.1029/2004JA010920.

Yue, X. A., W. S. Schreiner, D. C. Hunt, C. Rocken, and Y. H. Kuo (2011), Quantitative evaluation of the low Earth orbit satellite based slant total electron content determination, *Space Weather*, *9*, S09001, doi:10.1029/2011SW000687.

Zhao, B., W. Wan, and L. Liu (2005), Response of equatorial anomaly to the October–November 2003 superstorm, *Ann. Geophys.*, *25*, 1555–1568.

Zhao, B., W. Wan, J. Lei, Y. Wei, Y. Sahai, and B. Reinisch (2012), Positive ionospheric storm effects at Latin America longitude during the superstorm of 20–22 November 2003: Revisit, *Ann. Geophys.*, *30*, 831–840.

Zhong, J., J. Lei, X. Dou, and X. Yue (2015), Assessment of vertical TEC mapping functions for space-based GNSS observations, *GPS Solutions*, doi:10.1007/s10291-015-0444-6.